

Research Article

Surfactant-Free Solvothermal Method for Synthesis of Mesoporous Nanocrystalline TiO₂ Microspheres with Tailored Pore Size

Yajing Zhang, Sujuan Zhang, Kangjun Wang, Fu Ding, and Jing Wu

College of Chemical Engineering, Shenyang University of Chemical Technology, Shenyang 110142, China

Correspondence should be addressed to Fu Ding; dingfuschr@hotmail.com and Jing Wu; wujing7275@163.com

Received 24 January 2013; Accepted 9 March 2013

Academic Editor: Guo Gao

Copyright © 2013 Yajing Zhang et al. This is an open access article distributed under the Creative Commons Attribution License, which permits unrestricted use, distribution, and reproduction in any medium, provided the original work is properly cited.

TiO₂ mesoporous microspheres self-assembled from nanoparticles were synthesized by a surfactant-free solvothermal route. The TiO₂ precursors were fabricated by tetrabutyl titanate, glacial acetic acid, and urea in the ethanol solution at 140°C for 20 h, and TiO₂ mesoporous microspheres were obtained by a postcalcination at temperatures of 450°C for promoting TiO₂ crystallization and the removal of residual organics. The phase structure, morphology, and pore nature were characterized by XRD, SEM, and nitrogen adsorption-desorption measurements. The as-prepared TiO₂ microspheres are in anatase phase, with 2–3 μm in diameter, and narrow pore distribution range is 3–4 nm. The adjustments of the synthetic parameters lead to the formation of the mesoporous TiO₂ microspheres with tuned pore size distributions and morphology.

1. Introduction

The existence of a close relationship between specific morphologies and unique properties in nanomaterials has ignited much attention to the synthesis of novel nanostructures for a broad domain of applications in the past decade [1]. Due to its large surface area, networked pore distribution, and unique band structure, mesoporous TiO₂ has attracted explosive attention for photocatalytic applications, such as water splitting, water and air purification, antibacterial materials and sterilization [2, 3]. A lot of chemical synthetic methods have been developed for fabricating the TiO₂ nanomaterials, including sol-gel [4], hydrolysis [5], precipitation [6], and hydrothermal methods [7, 8]. Hydrothermal method has been widely used for preparing mesoporous TiO₂ owing to the controllable morphology and porous structure as well as the high crystallization degree of the product [9]. It is found that phase selection (rutile, anatase, or brookite), particle shape and size, and crystal orientation with specific lattice plane are controllable depending on synthetic conditions [10–12]. Nevertheless, few reports focus on the effect of synthetic

conditions on the pore size distribution. Most synthesis processes use template for the growth of anisotropic nanocrystals. Templates used include hard template (porous silica, alumina, or latex spheres, etc.) and soft template (triblock copolymer or surfactants) [13–15]. However, after synthesis, the template has to be removed from the sample to make the pores accessible. This can be achieved by thermal treatment (calcination) or solvents extraction [16]. In most cases, TiO₂ mesoporous materials are calcined; the thermal treatment processes frequently lead to the partial or total collapse of the porous structure during the template removal process and thus result in the decrease of the surface area [17]. In addition, some template cannot be completely removed by either calcination or solvent extraction because it tightly bound to the materials. Therefore, developing approaches without template and surfactant to overcome these limitations are highly demanded. Moreover, during the process of use, TiO₂ nanomaterials are subjected to the difficulties in handling and additional cost for recycling process; thus micro- and submicrometer scaled materials are often preferred in the large-scale production [18].

Here, mesoporous TiO₂ microspheres self-assembled from nanoparticles have been fabricated by a surfactant-free, convenient, and low-cost solvothermal method, which can conquer the issues above-mentioned. In addition, the diameters size, pore volume, BET surface areas, and the pore size distributions can also be tuned by adjusting synthesis parameters. This synthesis method can also be extended for the fabrication of other mesoporous metal oxide materials.

2. Experimental Section

2.1. Synthesis of Mesoporous Nanocrystalline TiO₂ Microspheres. All the reagents are analytical grade and were used without further purification (from Sinopharm Chemical Reagent Ltd.). In a typical procedure, 12 mmol urea was dissolved into 60 mL of absolute ethanol; then the solution was slowly added into the other solution (mixture of 20 mL ethanol, 2 mL tetrabutyl titanate (Ti(OC₄H₉)₄), and 1 mL glacial acetic acid (CH₃COOH)) under stirring. The solution was transferred into a 100 mL Teflon-lined autoclave after stirring for 30 min. The autoclave was put into an oven and maintained at 140 °C for 20 h. The precipitate was rinsed by ethanol for several times, dried at 90 °C for 12 h, and then calcined at 450 °C for 2 h. For comparison, different amounts of urea were added while keeping other reaction conditions constant.

2.2. Characterization of Mesoporous Nanocrystalline TiO₂ Microspheres. XRD measurements were performed on a Bruker D8 X-ray diffractometer with Cu-K α radiation ($\lambda = 1.54156 \text{ \AA}$) at a scan rate of 4° min^{-1} at 45 kV and 40 mA.

The N₂ adsorption-desorption isotherms of the TiO₂ microspheres were obtained at -196°C using a Quantachrome Autosorb 1-C. Before measurements, samples were degassed under vacuum at 300°C for 4 hours. The Brunauer-Emmett-Teller (BET) approach was used to calculate specific surface area of the sample by using adsorption data over the relative pressure range of 0.05–0.30. The Barrett-Joyner-Halenda (BJH) approach was employed to determine pore size distribution and average mesopore diameter by using desorption data of the isotherms.

SEM images were obtained on a JEOL JEM 6360 scanning electron microscope with accelerating voltage of 20 kV.

3. Results and Discussion

3.1. Textural Properties. Figure 1 shows the XRD patterns of the TiO₂ samples prepared with different amounts of urea. The strong and sharp peaks observed in Figure 1 confirm the catalysts are all well crystallized. For all samples, the diffraction peaks appear at 25.17° , 38.23° , 48.09° , 55.05° , 62.83° , 69.7° and 75.3° , all the peaks can be indexed to TiO₂ phase (Anatase, JCPDS 21-1272), which corresponds to (101), (004), (200), (105), (204), (116), and (215) planes, respectively. No diffraction peaks of rutile TiO₂ phase can be detected. The XRD results indicate the as-prepared TiO₂ is of high purity. Normally, the rutile phase is more stable than the anatase phase. Here, the as-prepared TiO₂ mesoporous microspheres

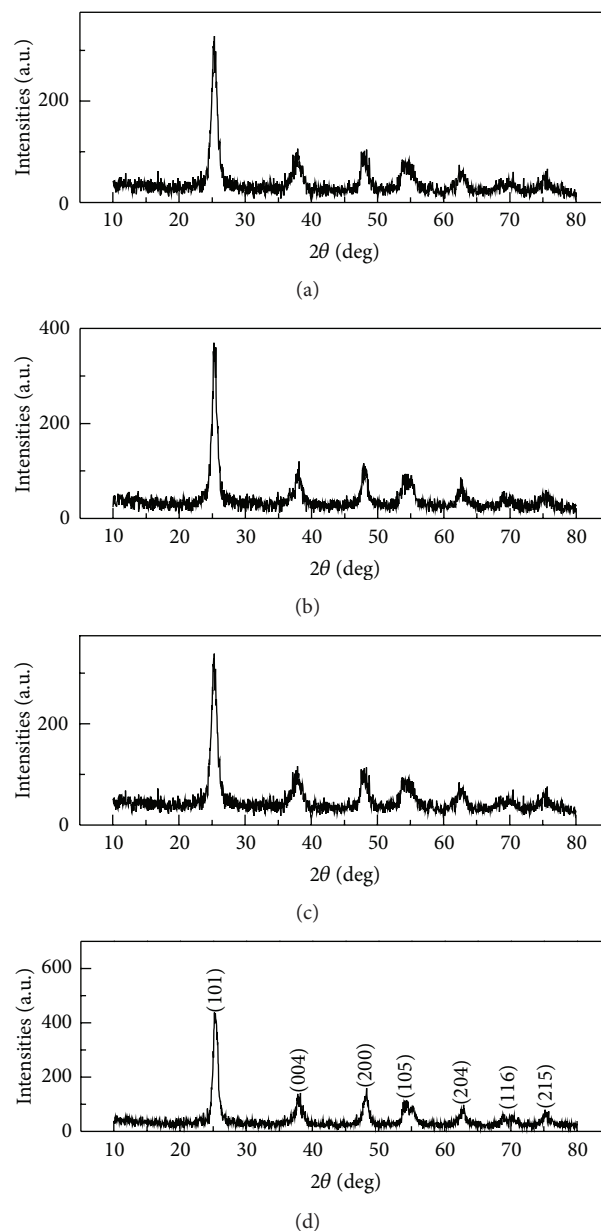


FIGURE 1: XRD patterns of mesoporous TiO₂ microspheres prepared with different amounts of urea: (a) 8 mmol; (b) 12 mmol; (c) 16 mmol; (d) 20 mmol.

are in anatase phase which could be ascribed not too high calcined temperature. The crystallite sizes of the synthesized TiO₂ samples estimated from the Debye-Scherrer equation [19], using the XRD line broadening of (101) diffraction peak, are reported in Table 1. It can be seen from Table 1 that crystallite sizes slightly decreased from 12.2 nm to 8.7 nm, with increasing the amount of urea, indicating the decrease of crystallization of the TiO₂ nanocrystals.

3.2. Morphology. The morphology and size of the TiO₂ samples were examined by SEM. Figures 2(a)–2(h) show that TiO₂ microspheres with different sizes can be achieved

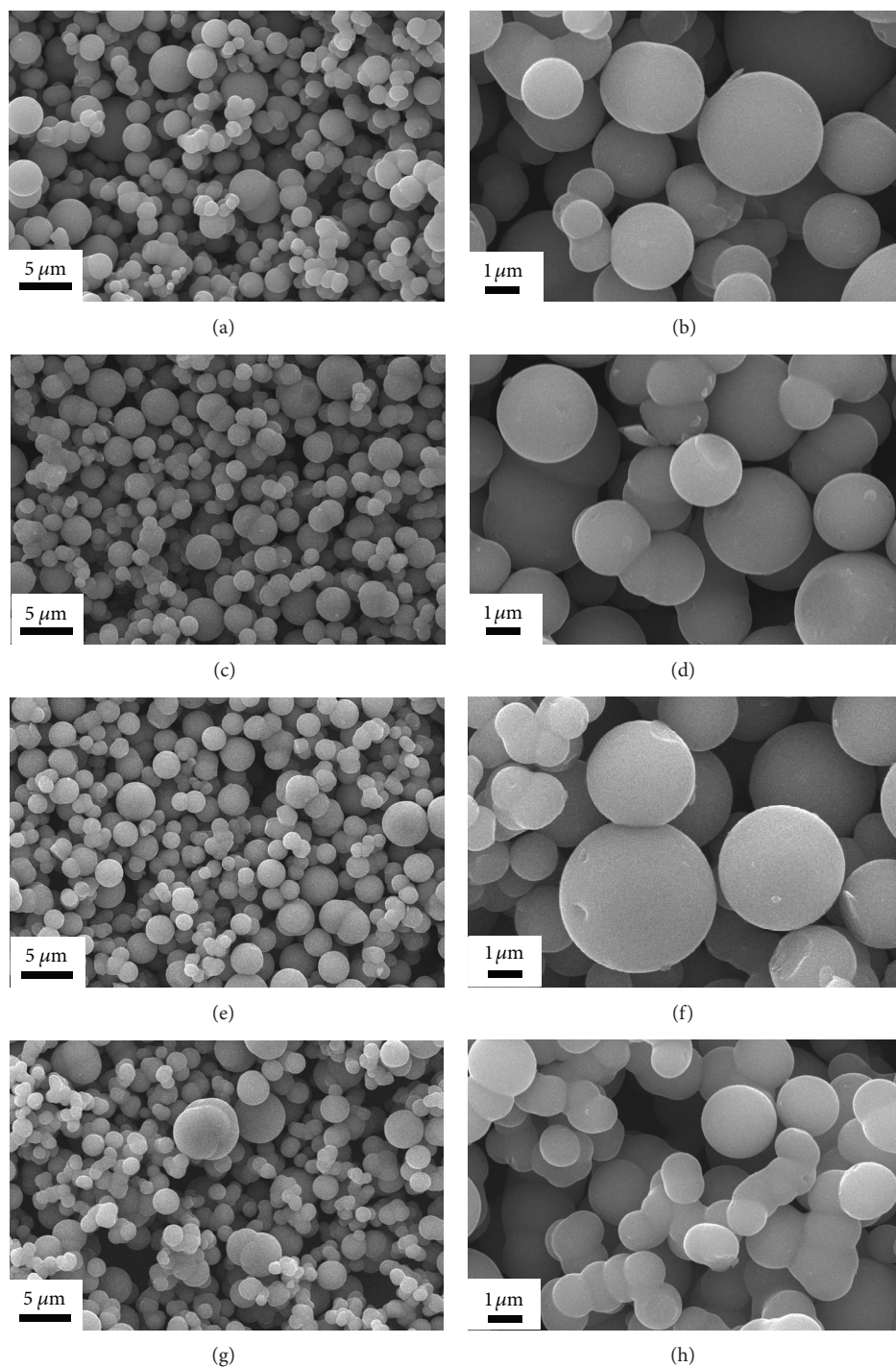


FIGURE 2: SEM images of mesoporous TiO_2 microspheres prepared with different amounts of urea: (a) 8 mmol; (b) 12 mmol; (c) 16 mmol; (d) 20 mmol.

accordingly by adjusting the amount of urea. When the amount of urea is 8 mmol, the size and surface structure of the microspheres can be observed in Figures 2(a) and 2(b). The TiO_2 microspheres are found to be 1–6 μm in diameter, the surfaces of the microspheres are very smooth, and the mean size of the diameter is about 4 μm . It is clearly seen that the microspheres disperse well, but the sizes are not

even. With the increasing amount of urea to 12 mmol (see Figures 2(c) and 2(d)), the mean diameter size of the TiO_2 microspheres decreases to about 2–3 μm , and the sizes are relatively uniform. The morphologies and sizes of the TiO_2 microspheres change little with increasing the urea amount to 16 mmol, as can be seen from Figures 2(e) and 2(f). However, if further increasing the urea amount to 20 mmol,

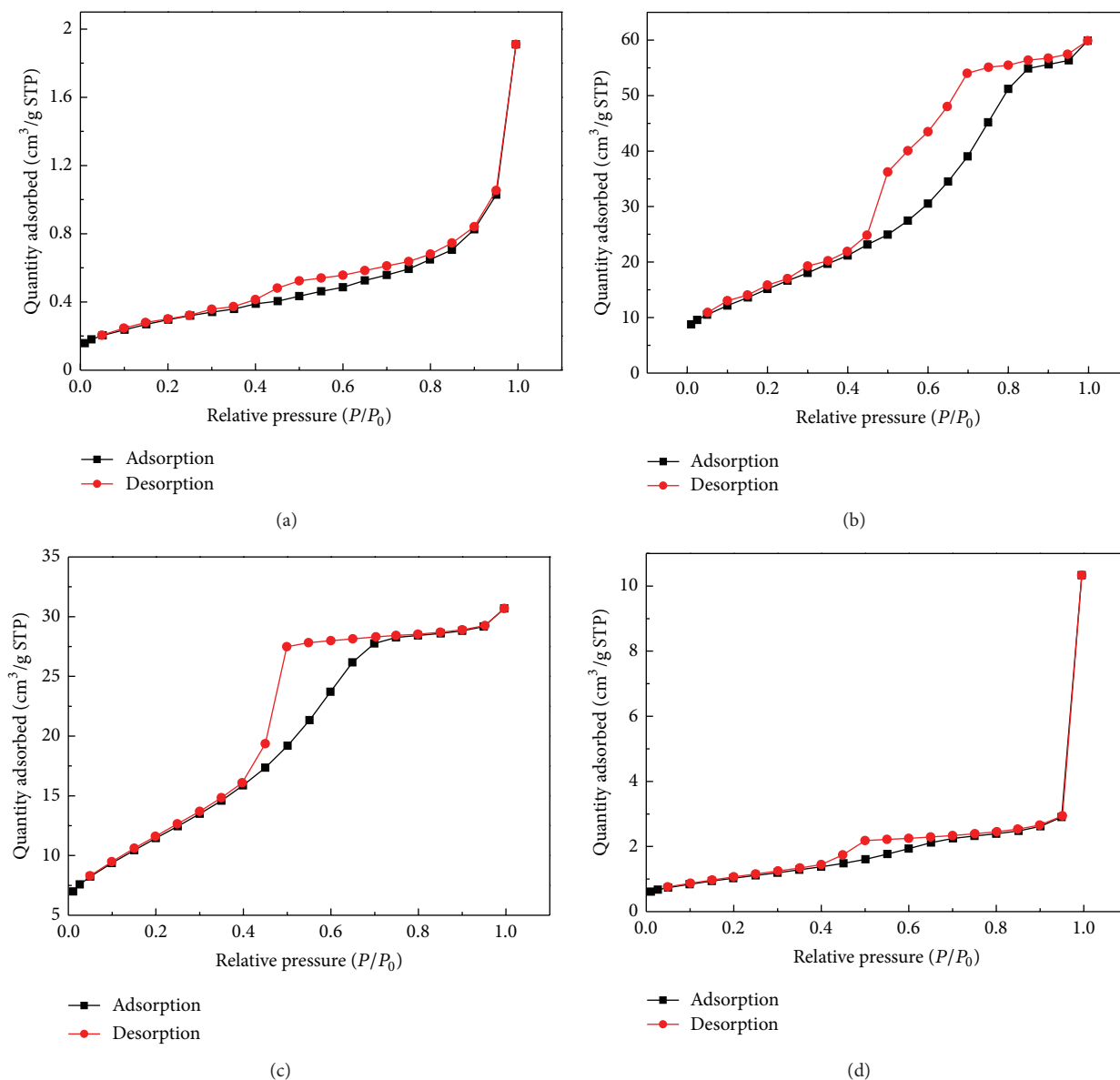


FIGURE 3: N_2 adsorption/desorption curves of mesoporous TiO_2 microspheres prepared with different amounts of urea: (a) 8 mmol; (b) 12 mmol; (c) 16 mmol; (d) 20 mmol.

it is observed from Figures 2(g) and 2(h) that “chain-like” and “peanut-like” TiO_2 microspheres are obtained, replacing the dispersed microspheres; the diameter sizes of the microspheres decrease, ranging from 1 to $3 \mu m$ again. The result means that the amount of the urea can greatly affect the size of the products, and the size of the microspheres decreased with increasing the amount of urea. Interestingly, the microspheres structure can still maintain the morphology even after ultrasonication for 30 min, indicating the structure is stable.

3.3. Specific Surface Area and Pore Character of the TiO_2 Microspheres. The microstructural characteristics of the TiO_2 microspheres were further investigated with the N_2

adsorption/desorption analysis. The adsorption isotherms of the TiO_2 microspheres are shown in Figures 3(a)–3(d), respectively. All samples exhibit type IV adsorption isotherms with different types of hysteresis loop (lines in Figures 3(a) and 3(d) with type H_3 , while lines in Figures 3(b) and 3(c) with type H_2), typical for mesoporous materials [20]. Usually, isotherms with type H_3 hysteresis loop means the occurrence of irregular long and narrow pores, while with type H_2 hysteresis loop mean the occurrence of regular “bottle-like” pores which exhibit a smaller size of opening but a larger size of inside chamber. With small amount of urea (8 mmol), the hysteresis loop ranges $P/P_0 = 0.4 - 0.85$; when $P/P_0 = 0.9 - 1$, the adsorption increases significantly, indicating the existence of macropores with diameter of 10–100 nm [21]. This speculation can also be proved from the

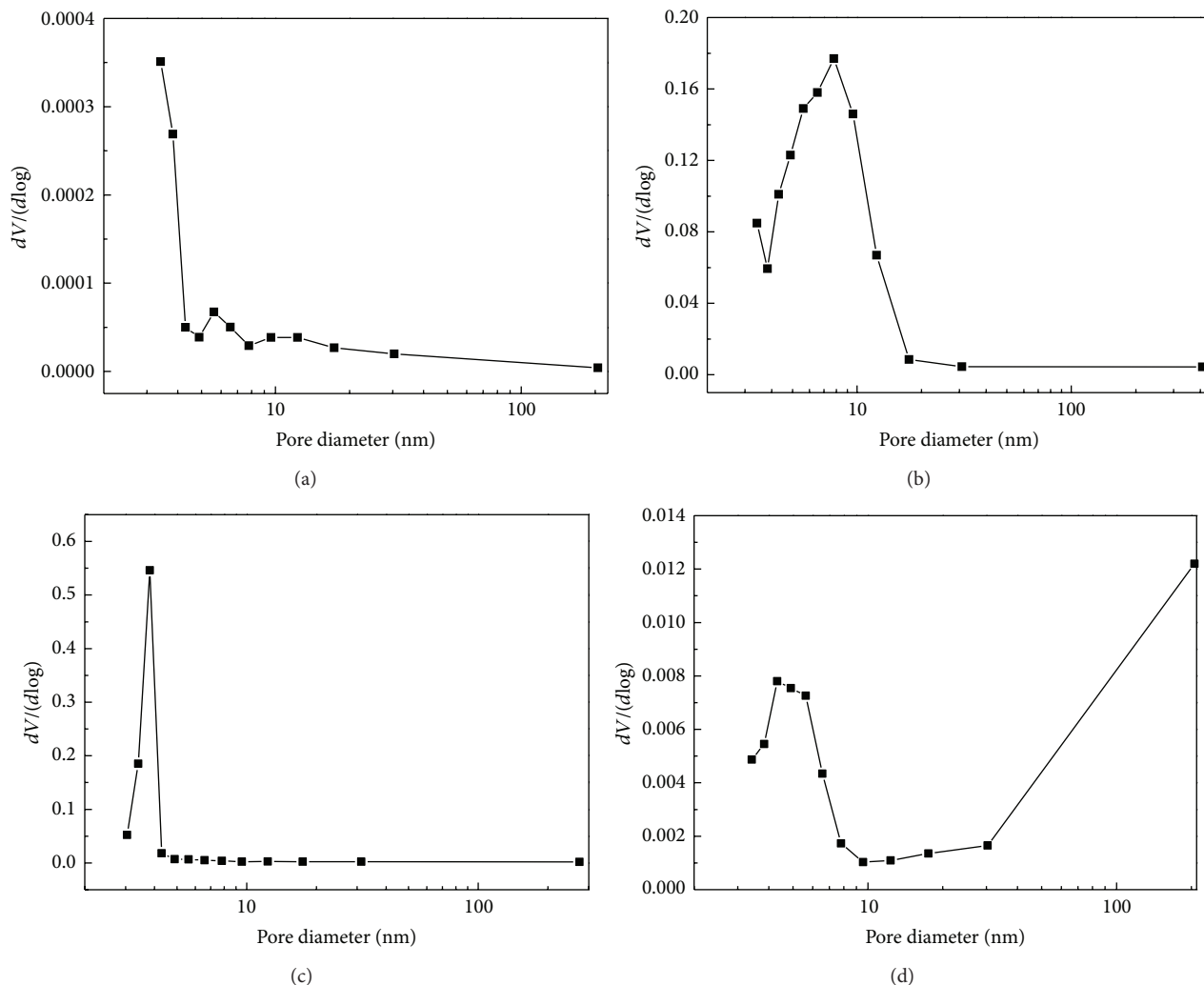


FIGURE 4: Pore size distributions of mesoporous TiO_2 microspheres prepared with different amounts of urea: (a) 8 mmol; (b) 12 mmol; (c) 16 mmol; (d) 20 mmol.

TABLE 1: Textural and structural parameters of mesoporous TiO_2 samples prepared with different amounts of urea.

Urea (mmol)	Phase	Crystallite size ^a (nm)	BET surface area ^b (m^2/g)	Pore volume ^c (cm^3/g)	Average pore diameter ^d (nm)
8	Anatase	12.2	1.09	0.002	3.5
12	Anatase	10.4	57.35	0.085	5.6
16	Anatase	9.2	42.45	0.045	3.8
20	Anatase	8.7	3.76	0.015	4.3

^aCrystallite size was calculated from the Scherrer equation based on the diffraction peak (101). ^bThe specific surface area was calculated by BET method. ^cThe total pore volume is taken from the adsorption branch of the nitrogen isotherm curve. ^dThe average pore diameter is estimated using the adsorption branch of the isotherm and BJH model.

corresponding wide pore size distribution as depicted in Figure 4(a). When the amount of urea increased to 12 mmol, the hysteresis loop also ranges $P/P_0 = 0.4 - 0.85$; at $P/P_0 = 0.9 - 1$, the adsorption increases little, implying almost all mesoporous structure of the sample. The pore size distributes 3–20 nm, as depicted in Figure 4(b). If further increasing the amount of urea; for example, 16 mmol urea were used,

and the hysteresis loop range of the sample also becomes narrow, only $P/P_0 = 0.4 - 0.75$, which demonstrates the pore size distribution is relatively concentrated, as can be seen from Figure 4(c), ranging only 3–4 nm. However, with more amount of urea (20 mmol), although the hysteresis loop still exhibits a small triangular shape and a steep desorption branch like the sample prepared with 16 mmol, the pore size

distribution becomes wide again. As indicated in Figure 4(d), there are two kinds of pore sizes, one is about 3–10 nm, and another is much larger than 30 nm (30–200 nm). It can be concluded that the amount of urea has a great influence on the pore size distribution of TiO₂ microspheres. This result can be explained from the point view of the nucleation and growth process of the TiO₂ microspheres. In our synthesis, urea can provide basic environment for the alcoholysis of Ti(OC₄H₉)₄ to Ti(OH)₄ and corresponding condensation. The overall growth mechanism of the TiO₂ precursors could be divided into two stages: the initial formation of nuclei and the subsequent growth of nuclei. When the amount of urea is too small, the alcoholysis rate is considerably slower, which can incur the greater difference of the growth times for the particle; so the diameter size uniformity of the product is poor. In contrast, if the amount of urea is too large, the alcoholysis rate is fast enough so that all nuclei are formed at the initial stage, and nearly null particles are available for the subsequent nuclei growth. Accordingly, the nuclei aggregate to become spheres driven by minimization of surface energies according to the Gibbs-Thomson law; therefore the bigger microspheres grow up at the expense of disappearance of smaller ones, and the diameter size distribution is also poor. In addition, the amount of urea influences the condensation rate of Ti(OH)₄, and the narrow pore size distribution can be obtained at suitable condensation rate. Our research results indicate nanocrystalline TiO₂ mesoporous microspheres with controlled pore size distribution which can be synthesized by controlling the amount of urea.

It is also interesting to note that BET specific surface areas, pore volumes, and average pore diameters also changed with the amount of urea used in preparation, as shown in Table 1. The BET specific surface areas and pore volumes first increase and then decrease with the increasing amount of urea. The TiO₂ samples prepared with 12 mmol urea exhibit the maximum BET surface area of 57.35 m²/g, which is a little larger than that of commercial P25 [22].

4. Conclusions

In summary, mesoporous TiO₂ microspheres self-assembled from nanoparticles are synthesized by a surfactant-free Solvothermal method combined with postcalcination route. The as-prepared TiO₂ microspheres show anatase phase, high degree of crystallinity, and large BET surface areas. By adjusting the amount of urea used in synthesis, the pore size distribution and the diameters of the mesoporous TiO₂ microspheres can be tuned. The new approach could be extended to the fabrication of other metal mesoporous materials.

Acknowledgment

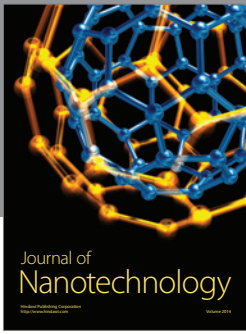
The authors thank Liaoning Science and Technology Department Foundation (no. 2007223016), Liaoning Educational Department Foundation (L2011065), Shenyang Science and Technology Department Foundation (no. F11-264-1-76), and

Scientific Research Starting Foundation for Doctor, Liaoning Province (no. 20111046), for financial support.

References

- [1] Y. J. Zhang, S. W. Or, and Z. D. Zhang, "Hydrothermal self-assembly of hierarchical cobalt hyperbranches by a sodium tartrate-assisted route," *RSC Advances*, vol. 1, no. 7, pp. 1287–1293, 2011.
- [2] J. Y. Cho, W. H. Nam, Y. S. Lim, W.-S. Seo, H.-H. Park, and J. Y. Lee, "Bulky mesoporous TiO₂ structure," *RSC Advances*, vol. 2, pp. 2449–2453, 2012.
- [3] A. Wold, "Photocatalytic properties of TiO₂," *Chemistry of Materials*, vol. 5, no. 3, pp. 280–283, 1993.
- [4] D. M. Antonelli and J. Y. Ying, "Synthesis of hexagonally packed mesoporous TiO₂ by a modified sol-gel method," *Angewandte Chemie*, vol. 34, no. 18, pp. 2014–2017, 1995.
- [5] P. Kubiak, J. Geserick, N. Hüsing, and M. Wohlfahrt-Mehrens, "Electrochemical performance of mesoporous TiO₂ anatase," *Journal of Power Sources*, vol. 175, no. 1, pp. 510–516, 2008.
- [6] D. Dambournet, I. Belharouak, and K. Amine, "Tailored preparation methods of TiO₂ anatase, rutile, brookite: mechanism of formation and electrochemical properties," *Chemistry of Materials*, vol. 22, no. 3, pp. 1173–1179, 2010.
- [7] F. Liu, C.-L. Liu, B. Hu, W.-P. Kong, and C.-Z. Qi, "High-temperature hydrothermal synthesis of crystalline mesoporous TiO₂ with superior photo catalytic activities," *Applied Surface Science*, vol. 258, no. 19, pp. 7448–7454, 2012.
- [8] K. H. Lee and S. W. Song, "One-step hydrothermal synthesis of mesoporous anatase TiO₂ microsphere and interfacial control for enhanced lithium storage performance," *ACS Applied Materials & Interfaces*, vol. 3, no. 9, pp. 3697–3703, 2011.
- [9] Z. Bian, J. Zhu, F. Cao, Y. Huo, Y. Lu, and H. Li, "Solvothermal synthesis of well-defined TiO₂ mesoporous nanotubes with enhanced photocatalytic activity," *Chemical Communications*, vol. 46, no. 44, pp. 8451–8453, 2010.
- [10] Y. Zhang, L. Wu, Q. Zeng, and J. Zhi, "An approach for controllable synthesis of different-phase titanium dioxide nanocomposites with peroxotitanium complex as precursor," *Journal of Physical Chemistry C*, vol. 112, no. 42, pp. 16457–16462, 2008.
- [11] M. G. Choi, Y. G. Lee, S. W. Song, and K. M. Kim, "Lithium-ion battery anode properties of TiO₂ nanotubes prepared by the hydrothermal synthesis of mixed (anatase and rutile) particles," *Electrochimica Acta*, vol. 55, no. 20, pp. 5975–5983, 2010.
- [12] A. R. Armstrong, G. Armstrong, J. Canales, and P. G. Bruce, "TiO₂-B nanowires," *Angewandte Chemie*, vol. 43, no. 17, pp. 2286–2288, 2004.
- [13] M. Alvaro, C. Aprile, M. Benitez, E. Carbonell, and H. Garcia, "Photocatalytic activity of structured mesoporous TiO₂ materials," *Journal of Physical Chemistry B*, vol. 110, no. 13, pp. 6661–6665, 2006.
- [14] H. Shibata, T. Ogura, T. Mukai, T. Ohkubo, and H. Sakai, "Direct synthesis of mesoporous titania particles having a crystalline wall," *Journal of the American Chemical Society*, vol. 127, no. 47, pp. 16396–16397, 2005.
- [15] S. Li, Q. Shen, J. Zong, and H. Yang, "Synthesis of size-tunable mesoporous anatase titania spheres by a template-free method," *Materials Research Bulletin*, vol. 45, no. 7, pp. 882–887, 2010.
- [16] K. Yoo, H. Choi, and D. D. Dionysiou, "Ionic liquid assisted preparation of nanostructured TiO₂ particles," *Chemical Communications*, vol. 10, no. 17, pp. 2000–2001, 2004.

- [17] J. Wang, Y. Zhou, Y. Hu, R. O'hayre, and Z. Shao, "Facile synthesis of nanocrystalline TiO₂ mesoporous microspheres for lithium-ion batteries," *Journal of Physical Chemistry C*, vol. 115, no. 5, pp. 2529–2536, 2011.
- [18] S. K. Das, M. Patel, and A. J. Bhattacharyya, "Effect of nanostructuring and ex situ amorphous carbon coverage on the lithium storage and insertion kinetics in anatase titania," *ACS Applied Materials and Interfaces*, vol. 2, no. 7, pp. 2091–2099, 2010.
- [19] Y. J. Kim, S. Y. Chai, and W. I. Lee, "Control of TiO₂ structures from robust hollow microspheres to highly dispersible nanoparticles in a tetrabutylammonium hydroxide solution," *Langmuir*, vol. 23, no. 19, pp. 9567–9571, 2007.
- [20] S. Lowell, J. E. Shields, and M. A. Thomas, *Characterization of Porous Solids and Powders: Surface Area, Pore Size and Density*, Kluwer Academic Publishers, Dordrecht, The Netherlands, 2004.
- [21] G. Calleja, D. P. Serrano, R. Sanz, P. Pizarro, and A. García, "Study on the synthesis of high-surface-area mesoporous TiO₂ in the presence of nonionic surfactants," *Industrial and Engineering Chemistry Research*, vol. 43, no. 10, pp. 2485–2492, 2004.
- [22] S. Sakulkaemaruethai and T. Sreethawong, "Synthesis of mesoporous-assembled TiO₂ nanocrystals by a modified urea-aided sol-gel process and their outstanding photocatalytic H₂ production activity," *International Journal of Hydrogen Energy*, vol. 36, no. 11, pp. 6553–6559, 2011.



Hindawi

Submit your manuscripts at
<http://www.hindawi.com>

